

Model-building study of the combining sites of two antibodies to $\alpha(1\rightarrow6)$ dextran

(cavity-type site/groove-type site/length of complementarity-determining regions)

EDUARDO A. PADLAN* AND ELVIN A. KABAT†‡

*Laboratory of Molecular Biology, National Institute of Diabetes and Digestive and Kidney Diseases, National Institutes of Health, Bethesda, MD 20892; †Departments of Microbiology, Genetics and Development, and Neurology, and the Cancer Center/Institute of Cancer Research, College of Physicians and Surgeons, Columbia University, New York, NY 10032; and ‡National Institute of Allergy and Infectious Diseases, National Institutes of Health, Bethesda, MD 20892

Contributed by Elvin A. Kabat, April 1, 1988

ABSTRACT Models of the Fv portion (containing the variable regions of the heavy and light chains) of two monoclonal anti- $\alpha(1\rightarrow6)$ dextran antibodies, W3129 and 19.1.2, were constructed from amino acid sequences and the known three-dimensional structures of the Fv portions of McPC603 and J539. The modeled combining site of W3129 has a protrusion on one side, formed by the long complementarity-determining region 1 of the light chain and the long complementarity-determining region 3 of the heavy chain, and has a cavity accommodating a glucose moiety. The model of the 19.1.2 site is basically flat with a shallow groove that can accommodate several internal glucose units. These results support the earlier conclusions, from ligand binding data, that W3129 has a cavity-type site, involving the terminal nonreducing glucose residue (endbinder), whereas 19.1.2 has a groove-type site.

In 1975, Cisar *et al.* (1) studied the fine structure of the combining sites of two murine monoclonal IgA anti- $\alpha(1\rightarrow6)$ dextran antibodies, W3129 and QUPC52. The W3129 site was saturated by isomaltopentaose and that of QUPC52 by isomaltohexaose. Surprisingly, the association constant (K_a) of W3129 was 20-fold higher than that of QUPC52 ($1.7 \times 10^5 \text{ M}^{-1}$ by equilibrium dialysis and fluorescence quenching vs. $8.4 \times 10^3 \text{ M}^{-1}$ by equilibrium dialysis). This was unexpected, since the K_a usually is correlated with site size. By equilibrium dialysis displacement of [^3H]isomaltoheptitol by methyl α -D-glucoside and isomaltose, these ligands were found to have K_a values of 9.4×10^2 and $1.6 \times 10^3 \text{ M}^{-1}$, respectively, with W3129, whereas with QUPC52 the values were barely measurable (values of about 16 M^{-1} were found). This finding was interpreted as indicating that W3129 was specific for the terminal nonreducing end of the oligosaccharide antigen [an endbinder (2)], or cavity-type site (1), whereas QUPC52 was hypothesized to have a groove-type site not involving the nonreducing end of the $\alpha(1\rightarrow6)$ -linked glucose chain. This was readily confirmed by using a linear dextran of 200 $\alpha(1\rightarrow6)$ -linked glucose units (3) with but one nonreducing end. Since the linear dextran was monovalent, it did not precipitate W3129, but it inhibited precipitation of W3129 by multivalent native dextran, as would be expected. Toward QUPC52, with specificity for an extended internal chain of $\alpha(1\rightarrow6)$ -linked glucoses, the linear dextran would be multivalent and precipitated with QUPC52 (1). This distinction has been supported by fluorescence quenching data (1, 4).

The amino acid sequence of W3129 has been deduced from cDNA (5), but the sequence of QUPC52 has not been determined. However, many hybridoma proteins with

groove-type sites have been sequenced (6). One of these, 19.1.2, has a combining-site size complementary to an internal sequence of seven $\alpha(1\rightarrow6)$ -linked glucose units and a K_a for isomaltoheptaose of $8.1 \times 10^3 \text{ M}^{-1}$. Its light-chain variable region (V_L) (6) has the germ-line sequence of V_{κ} -OX1 (7, 8) and its heavy-chain variable region (V_H) belongs to the J558 family (9, 10).

We attempted to make molecular models of these two types of anti- $\alpha(1\rightarrow6)$ dextran combining sites to ascertain whether they would provide any support for the distinction between a cavity-type site, or endbinder, and a groove-type site (1). The results show a striking difference between W3129 and 19.1.2; W3129 has a cavity that can accommodate a terminal nonreducing glucose residue, whereas 19.1.2 has a shallow groove accommodating several glucose residues. The cavity in W3129 is formed by the presence of amino acids with smaller side chains than those in 19.1.2; the side chains of 19.1.2 effectively close or fill-in the cavity. Differences in lengths of the complementarity-determining regions (CDRs) also contribute significantly to the differences in the topography of the combining sites.

MATERIALS AND METHODS

Amino Acid Sequences. The amino acid sequences for the V_L and V_H of protein W3129 were from Borden and Kabat (5), those for the monoclonal antibody 19.1.2 were from Akolkar *et al.* (6), and those for the McPC603 and J539 proteins were from the compilation of Kabat *et al.* (11). The sequences of the CDRs of these proteins are compared in Fig. 1. The numbering scheme used here is that of Kabat *et al.* (11).

Atomic Coordinates for the Starting Models. The atomic coordinates for the V domains of McPC603 protein were from the structure of the McPC603 Fab fragment-phosphocholine complex refined at 3.1-Å resolution [E.A.P., G. H. Cohen, and D. R. Davies, unpublished data; available from the Protein Data Bank (13) (file no. 2MCP)]. The coordinates for J539 Fab were obtained from a structural analysis at 2.65-Å resolution (14). The J539 coordinates used (courtesy of T. N. Bhat, National Institutes of Health) were from the refinement stage where the crystallographic agreement factor R was 19.0%.

Model Building. The models of the Fv of W3129 and 19.1.2 proteins were built by using the interactive graphics program FRODO (15), adapted to an Evans and Sutherland PS300 system (16). Models of individual domains were built by assuming that the backbone structures of the homologous domains were the same except in regions where there are

Light chains:

	24	27abc	def	34	50	56	89	97
McPC603	KSSQSL	LNSGNQ	KNFLA	GASTRES	QNDHSY	PLT		
W3129	RSSQSL	ATS-HG	ITYLS	GISNRFS	LQGS	QPLA		
J539	SASS-----	SVSSLH		EISKLAS	QQW	PLIT		
19.1.2	SASS-----	SVSYMH		DTSKLAS	QQW	SNPYT		

Heavy chains:

	31	35	52abc	60	65	95	100abcdijk
McPC603	DFYME		ASRNKGNKYTTEYSASVKG			NYYGST----	WYFDV
W3129	RYWMS		EIN--PDSSTINYTPSLKD			LGGDLHYAM---	DY
J539	KYWMS		EIH--PDSGTINYTPSLKD			LHYGYN-----	AY
19.1.2	SYWIE		EIL--PGSGSTNYNEKFKG			HYYGSSSF-----	AY

FIG. 1. Amino acid sequences of the CDRs of McPC603, W3129, J539, and 19.1.2 immunoglobulins, shown in the one-letter amino acid code (12). Residues 27a-f, 52a-c, and 100a-d and i-k are identified by lowercase letters to avoid confusion with the uppercase letters representing the amino acids. In W3129, residue 96 of the light chain was mistranslated (5) from the nucleotide sequence and should be leucine as given here instead of serine.

length differences (17). Only in the CDRs are there length differences (Fig. 1), and the starting models for the various CDRs were chosen according to sequence and length similarity.

The backbone dihedral angles of the starting models were preserved except in the regions where insertions and deletions were required. Whenever the backbone had to be

restructured, only energetically acceptable main-chain torsional angles were used. Every effort was made to retain the side-group torsional angles of the starting models as well. However, when the side group in the starting model was replaced by one that was structurally dissimilar, then one of the energetically preferred torsional angles was used. The angle chosen was that allowing the new side group to lie as

Table 1. Conformational torsion angles in the CDRs of the W3129 Fv model before energy minimization

CDR	Residue	Angle, degrees							CDR	Residue	Angle, degrees						
		ϕ	ψ	χ^1	χ^2	χ^3	χ^4	χ^5			ϕ	ψ	χ^1	χ^2	χ^3	χ^4	χ^5
1-L	R 24	-108	149	15	-159	167	67	0	2-H	E 50	-129	150	-135	-170	179		
	S 25	-114	154	46						I 51	-139	136	179	156			
	S 26	-80	-10	75						N 52	-61	144	-155	180*			
	Q 27	-143	139	-119	138	-105				P 52C	-39	-38	-31	31	-17		
	S 27A	-51	137	-172						D 53	-116	49	-82	74			
	L 27B	-105	-19	-69	178					S 54	40	10	-30				
	A 27C	-72	131							S 55	-72	-35	180*				
	T 27D	-85	170	-129						T 56	-126	125	-44				
	S 27E	-97	33	60*						I 57	-124	121	-72	135			
	H 28	-115	-12	-60*	-90*					N 58	-109	141	-67	125			
	G 29	73	83							Y 59	-127	159	-74	-85			
	I 30	-166	131	-60*	-180*					T 60	-77	116	-76				
	T 31	-96	150	-15						P 61	-43	-42	-13	6	2		
	Y 32	-101	66	-59	37					S 62	-54	-34	106				
L 33	-127	128	175	142				L 63	-98	-11	-57	172					
S 34	-117	154	180*					K 64	-44	-35	-65	175	179	-105			
2-L	G 50	66	-159						D 65	-85	19	-91	-154				
	I 51	-98	-20	180*	180*				3-H	L 95	-100	90	-156	60*			
	S 52	-123	-9	52				G 96		-76	154						
	N 53	-72	116	-51	180			G 97		164	115						
	R 54	-84	130	174	-132	-56	-9	-178		D 98	-159	-46	-180*	180*			
	F 55	-68	142	179	90*					L 99	-74	-56	-60*	60*			
	S 56	-50	132	-173						H 100	-132	-139	-60*	90*			
								Y 100A		-57	178	60*	90*				
3-L	L 89	-139	155	140	60*				Y 100B	-104	140	-57	89				
	Q 90	-96	104	133	180*	-180*			A 100C	-168	162						
	G 91	-103	29						M 100D	-95	106	-59	180*	180*			
	S 92	-81	-64	-172					D 101	-71	-47	104	-76				
	H 93	-153	158	48	90*				Y 102	-128	129	-60*	-90*				
	Q 94	-70	140	-66	180*	180*											
	P 95	-76	139	-20	44	-50											
	L 96	-65	146	-73	17												
A 97	-134	157															
1-H	R 31	-77	-55	-109	-133	-64	-179	0									
	Y 32	-89	157	177	46	-108											
	W 33	-81	142	-80	75												
	M 34	-127	155	-67	-54	-70											
	S 35	-143	170	32													

The energetically preferred torsion angles used in the model building (± 60 or 180 degrees for aliphatic groups, ± 90 degrees for aromatic groups) are indicated by asterisks. Otherwise, the conformational angles are those of the starting model.

close as possible to the position of the replaced side group without resulting in severe steric contacts. The torsional angles in the CDRs of the Fv fragments of W3129 and 19.1.2 after modeling are listed in Tables 1 and 2.

The amino acid sequence of W3129 V_L is slightly more similar to McPC603 V_L than to J539 V_L. Moreover, W3129 and McPC603 both have proline at position 95, whereas J539 has a proline at position 94, causing the third CDR of the light chain (CDR3-L) of J539 to trace a slightly different course (14). Pro-95 in McPC603 is in the cis configuration (18), which was retained for Pro-95 of W3129. CDR1-L of W3129 is one residue shorter than that of McPC603 but six residues longer than that of J539 (Fig. 1). Accordingly, McPC603 V_L was the starting model for W3129 V_L. Residue 27f (Fig. 1) was excised from the McPC603 CDR1-L loop and the severed ends were rejoined.

The amino acid sequence of W3129 V_H is almost identical to that of J539 even in the heavy-chain CDRs CDR1-H and CDR2-H, so that J539 V_H was the starting model for W3129 V_H. However, in CDR3-H, W3129 is closer in length to McPC603 than to J539. Accordingly, CDR3-H of McPC603 was the starting model for this region in W3129 with one residue inserted after Ser-99. The quaternary structure of McPC603 Fv was assumed for W3129.

The amino acid sequence of 19.1.2 V_L is more like that of J539 V_L even in the CDRs (Fig. 1). Since, as in W3129, there is a proline at position 95, the starting model for 19.1.2 V_L was that of J539 with the last five residues of CDR3-L replaced by the corresponding region of McPC603.

The amino acid sequence of 19.1.2 V_H is also more like that of J539 (Fig. 1), which served as the starting model for this domain. However, CDR3-H is one residue shorter than CDR3-H of McPC603 but one residue longer than that of J539. CDR3-H of McPC603 was chosen as the starting model for the CDR3-H of 19.1.2, with residue 100 excised. The quaternary structure of J539 Fv was assumed for 19.1.2.

The resulting models for the Fv portions of W3129 and 19.1.2 were energy-minimized by the program CHARMM (19) (courtesy of Eric Henry, National Institutes of Health). After 200 energy-minimization steps, the potential energy of the W3129 model was reduced from an initial value of 29,957 to -8,568 kcal/mol and that of the 19.1.2 model from 191,491 to -8,243 kcal/mol (1 kcal = 4184 J). The coordinates of the starting and energy-minimized models have been deposited in the Protein Data Bank (13) (file nos. 1FVB, 2FVB, 1FVW, and 2FVW).

RESULTS

The models for the Fv of W3129 and 19.1.2 are in Fig. 2 A and C. The surface representations (20) of the proposed combining sites are in Fig. 2 B and D.

The proposed combining sites for W3129 and 19.1.2 are very different both in the lengths of the CDRs and in the nature of their amino acids. A wall is formed by the long CDR1-L and CDR3-H of W3129 that protrudes on one side of the combining site (Fig. 2 A and B). This protrusion is absent in the combining site proposed for the 19.1.2 antibody (Fig. 2 C and D), mainly because of the much shorter CDR1-L of 19.1.2 [actually the shortest CDR1-L known (11)].

The combining-site surface proposed for 19.1.2 is relatively flat with a shallow groove (Fig. 2D), whereas that proposed for W3129 has a cavity in the middle (Fig. 2B). This cavity results principally from the presence of smaller residues at positions 91 and 96 in CDR3-L (glycine and leucine, respectively). In 19.1.2, these positions are occupied by tryptophan and tyrosine, respectively, and their bulky side groups effectively prevent the formation of a cavity like the one proposed for W3129.

Table 2. Conformational torsion angles in the CDRs of the 19.1.2 Fv model before energy minimization

CDR	Residue	Angle, degrees					
		ϕ	ψ	χ^1	χ^2	χ^3	χ^4
1-L	S 24	-125	146	32			
	A 25	-106	154				
	S 26	-82	-5	82			
	S 27	-174	163	71			
	S 29	-54	133	-84			
	V 30	-121	155	-60*			
	S 31	-78	-29	-49			
	Y 32	-161	168	-60*	-90*		
	M 33	-151	142	-173	-180*	-180*	
	H 34	-140	166	-25	-88		
2-L	D 50	-125	68	-89	180*		
	T 51	78	-37	136			
	S 52	-142	5	50			
	K 53	-87	128	-59	-166	164	108
	L 54	-75	117	-84	-155		
	A 55	-61	177				
	S 56	-44	-70	-124			
3-L	Q 89	-156	133	-174	-130	-78	
	Q 90	-103	160	60	93	-163	
	W 91	-135	108	166	69		
	S 92	-133	-68	-180*			
	S 93	-165	165	60*			
	N 94	-69	162	-60*	180*		
	P 95	-76	139	-20	44	-50	
	Y 96	-65	146	-73	-90*		
1-H	S 31	-77	-55	-109			
	Y 32	-89	158	-46	-108		
	W 33	-81	142	-80	75		
	I 34	-127	155	-67	-54		
	E 35	-143	170	32	180*	-180*	
	2-H	E 50	-129	150	-135	-170	179
I 51		-139	136	179	156		
L 52		-61	144	-155	60*		
P 52C		-39	-38	-31	31	-17	
G 53		-116	49				
S 54		40	10	-30			
G 55		-72	-35				
S 56		-126	125	-44			
T 57		-124	121	-72			
N 58		-109	141	-67	125		
Y 59		-127	159	-74	-85		
N 60		-77	116	-76	180*		
E 61		-43	-42	-180*	-180*	180*	
K 62		-54	-34	106	180*	180*	180*
F 63	-98	-11	-57	-90*			
3-H	K 64	-44	-35	-65	175	179	-105
	G 65	-85	19				
	H 95	-84	91	-180*	90*		
	Y 96	-73	119	-172	-88		
	Y 97	-62	172	60*	-90*		
	G 98	145	-40				
	S 99	-166	-95	180*			
	S 100	-155	121	-60*			
	S 100A	-168	175	60*			
	F 100B	-133	106	-59	175		
A 101	-71	-47					
Y 102	-128	123	-60*	90*			

See legend to Table 1.

The cavity in the model of W3129 Fv can accommodate a glucose moiety when inserted end-on (data not shown).

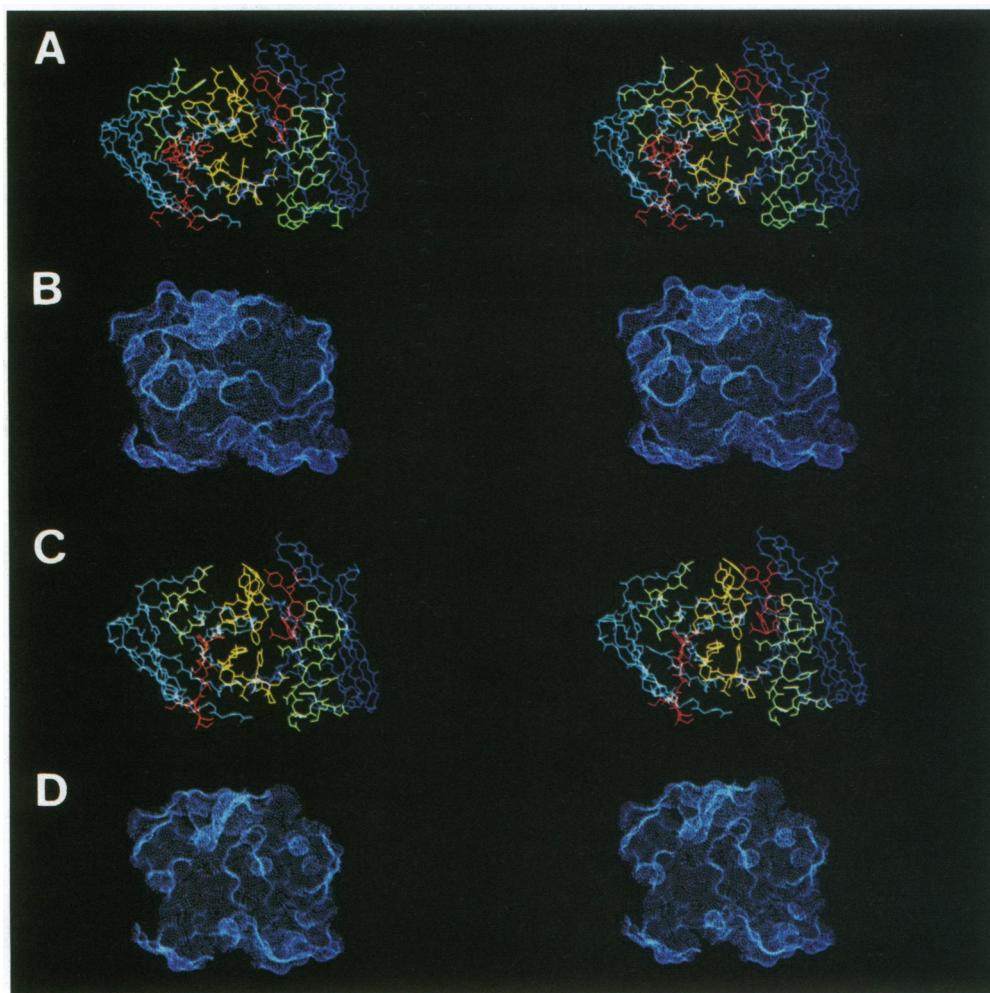


FIG. 2. Stereodrawings of the proposed combining sites of the anti- $\alpha(1\rightarrow6)$ dextran antibodies W3129 and 19.1.2. (A) The α -carbon backbone of the Fv of W3129. (B) The molecular surface (20) covering the combining site of W3129. (C) The α -carbon backbone of the Fv of 19.1.2. (D) The molecular surface covering the combining site of 19.1.2. V_L is on the left (light blue in A and C) and V_H is on the right (darker blue in A and C). CDR1-L and CDR1-H are shown in red, CDR2-L and CDR2-H in green, and CDR3-L and CDR3-H in yellow.

Likewise, the groove in the proposed 19.1.2 combining site can accommodate several sugar residues.

DISCUSSION

Modeling of the Fv of W3129 and 19.1.2 was straightforward and followed the technique proposed earlier (17). We assumed (i) the same quaternary association of V_L and V_H as observed in McPC603 and J539, (ii) the same V_L and V_H domain structures as found in these proteins, (iii) the same backbone structures in the CDRs as those from McPC603 or J539 if they have the same number of residues, and (iv) the same torsional angles in the main chain and side groups as in the parent regions on which the model structures were based. These assumptions are justified because of the high similarity in sequence among McPC603, J539, W3129, and 19.1.2. Furthermore, the conservation of the tertiary structures of homologous immunoglobulin domains and of their mode of association is well known (2, 21–23). Moreover, the disposition of similar side groups in highly homologous proteins has been shown to be preserved (24).

The necessary insertions and excisions were chosen to be as inconsequential as possible. CDRs whose lengths were closest to those of the unknown structures were chosen as starting models and the general course of the parent polypeptide chain was followed as closely as possible. Even then, very little modeling was needed, since the length differences

involved only one residue in the entire Fv of 19.1.2 and in V_L and V_H of W3129.

A long CDR1-L and a long CDR3-H characterize the combining site of McPC603 (18), which has a cavity to accept the specific hapten phosphocholine. This combination is found in most of the other antibodies with anti-phosphocholine specificity (11), which probably have the same mode of hapten binding (25). The endbinder, W3129, also has a long CDR1-L and a long CDR3-H. This combination may be characteristic of antibodies with cavity-type antigen-binding sites; it is not found in any of the anti- $\alpha(1\rightarrow6)$ dextran antibodies that are known to have groove-type sites (6). While some of the anti- $\alpha(1\rightarrow6)$ dextran antibodies with groove-type sites have long CDR1-Ls, their heavy chains have very short CDR3-Hs of only four amino acids (6).

W3129 is thus far unique among anti- $\alpha(1\rightarrow6)$ dextran immunoglobulins in having a cavity-type combining site. The model thus supports the original conclusion of Cisar *et al.* (1) that the terminal nonreducing end is more firmly held and is consistent with its high K_a . A subsequent alternative explanation (26) proposed that the "disproportionately high K_a for W3129 with methyl α -D-glucoside need not mean 'that the terminal nonreducing end is more firmly held' but only that of 5 sugar-binding subsites of W3129 one has a substantially higher K_a (subsite) for its glucosyl residue and its location may or may not be internal or peripheral in the sequence of 5 subsites" (26). Since one has only limited information about

exact shapes of sites, this might also be correct in certain cases.

W3129 belongs to the V_{H441} (XRPC24) (5) germ-line gene family (9, 10); more than 95% of its amino acid sequence is the same as that of XRPC24, an anti- $\beta(1\rightarrow6)$ galactan; the 16 sequenced anti- $\alpha(1\rightarrow6)$ dextran with groove-type sites belong to three different V_H germ-line gene families, J558, J606, and 36-60 (6). The significance of this requires further study. J539, an anti- $\beta(1\rightarrow6)$ galactan with a bent groove-type site (14), also belongs to the V_{H441} germ-line gene family. CDR1-Ls in mouse V_{κ} group VI sequences, which include anti-oxazolones (8) and anti- $\beta(1\rightarrow6)$ galactans, all lack the seven residues 27a-f and 28 (11), that our model seems to require for a cavity-type site. In contrast, the anti-phosphocholine myeloma and hybridoma proteins in mouse V_{κ} groups I and II (11) all have residues 27a-f and 28 (group I) or 27a-e and 28 (group II) in CDR1-L.

In V_H , all the groove-type anti- $\alpha(1\rightarrow6)$ dextran hybridoma proteins sequenced have CDR3-H having 4, 7, 8, or 10 residues (11), whereas W3129 has a CDR3-H of 12 residues (5), as do many anti-phosphocholine myeloma and hybridoma proteins (subgroup IIIA) (11). One of these, McPC603, shown by x-ray crystallography to have a cavity-type site, has 11 residues in CDR3-H.

Site modeling has substantial uncertainties and limitations. Although significant progress has been made towards the prediction of the structure of antibody combining sites, no model has been proposed that is in agreement with a crystallographically determined structure (see, for example, refs. 27 and 28). The models proposed here are energetically reasonable; however, each represents but one of many possible structures. Nevertheless, the present findings of cavity- and groove-type sites are remarkably consistent with conclusions drawn from immunochemical mapping of the fine structures of anti- $\alpha(1\rightarrow6)$ dextran immunoglobulins (1). This gives us confidence that details from our models will be useful in explaining in structural terms the results of chemical studies of ligand-binding to anti- $\alpha(1\rightarrow6)$ dextran immunoglobulins (1, 26). When model-building principles are better understood so that combining-site structures can be predicted consistently and accurately, then the immunochemical determination of fine structures, such as was done on these two anti- $\alpha(1\rightarrow6)$ dextran antibodies (1), and modeling based upon such evidence would permit much more rapid progress in characterizing antibody combining sites of different specificities and in evaluating the effects of mutations, either spontaneous or deliberately induced by site-directed mutagenesis. These advantages would be especially valuable in the study of anti-carbohydrate combining sites because of their relative simplicity; anti-protein combining sites will undoubtedly present much more difficulty, since every portion of a protein antigenic surface is believed (29) potentially to be able to induce monoclonal antibodies toward which the epitopes may overlap from one hybridoma to another. Other immunochemical methods of site mapping by the use of various synthetic oligosaccharides, which have proven successful in defining the fine structures of the blood group I (30) and A and B (31-33) epitopes, and the recent use of fluorine-substituted sugars to probe the anti- $\beta(1\rightarrow6)$ galactan antibodies (34), when correlated with amino acid sequence, will permit further progress in this endeavor.

Kimura *et al.* (35) have recently sequenced three monoclonal antibodies, all specific for 3-fucosyllactosamine, Gal $\beta(1\rightarrow4)$ (Fuc $\alpha(1\rightarrow3)$)GlcNAc-R (R denotes unidentified sugars); they belong to the V_{H441} (XRPC24) germ-line gene family with diversity segment D-Q52 and joining segment J_{H4} and to V_{κ} 24B and J κ 1. As does W3129, they also have a long CDR1-L containing residues 27a-e and 28 and a CDR3-H of

nine residues. It will be of interest to see whether modeling studies will also show a cavity-type site for these molecules.

We thank Dr. Eric Henry for help in the use of the program CHARMM and Drs. David R. Davies and Cornelius P. J. Glaudemans for comments and discussions. This work was supported by Grant PCM8600778 from the National Science Foundation and Grant IR01-A119042 from the National Institute of Allergy and Infectious Diseases to E.A.K. and by Cancer Support Grant CA13696 to Columbia University.

- Cisar, J., Kabat, E. A., Dorner, M. M. & Liao, J. (1975) *J. Exp. Med.* **142**, 435-459.
- Davies, D. R. & Metzger, H. (1983) *Annu. Rev. Immunol.* **1**, 87-117.
- Ruckel, E. R. & Schuerch, C. (1966) *J. Am. Chem. Soc.* **88**, 2605-2606.
- Bennett, L. G. & Glaudemans, C. P. J. (1979) *Carbohydr. Res.* **72**, 315-319.
- Borden, P. & Kabat, E. A. (1987) *Proc. Natl. Acad. Sci. USA* **84**, 2440-2443.
- Akolkar, P. N., Sikder, S. K., Bhattacharya, S. B., Liao, J., Gruezo, F., Morrison, S. L. & Kabat, E. A. (1987) *J. Immunol.* **138**, 4472-4479, and erratum (1987) **139**, 3911.
- Sikder, S. K., Akolkar, P. N., Kaladas, P. M., Morrison, S. L. & Kabat, E. A. (1985) *J. Immunol.* **135**, 4215-4221.
- Griffiths, G. M., Berek, C., Kaartinen, M. & Milstein, C. (1984) *Nature (London)* **312**, 271-275.
- Brodeur, P. H. & Riblet, R. (1984) *Eur. J. Immunol.* **14**, 922-930.
- Dildrop, R. (1984) *Immunol. Today* **5**, 85-86.
- Kabat, E. A., Wu, T. T., Reid-Miller, M., Perry, H. M. & Gottesman, K. S. (1987) *Sequences of Proteins of Immunological Interest* (Natl. Inst. Health, Bethesda, MD), 4th Ed.
- IUPAC-IUB Joint Commission on Biochemical Nomenclature (1968) *J. Biol. Chem.* **243**, 3557-3559.
- Bernstein, F. C., Koetzle, T. F., Williams, G. J. B., Meyer, E. F., Jr., Brice, M. D., Rogers, J. R., Kennard, O., Shimanouchi, T. & Tasumi, M. (1977) *J. Mol. Biol.* **112**, 535-542.
- Suh, S. W., Bhat, T. N., Navia, M. A., Cohen, G. H., Rao, D. N., Rudikoff, S. & Davies, D. R. (1986) *Proteins: Struct. Funct. Genet.* **1**, 74-80.
- Jones, T. A. (1978) *J. Appl. Crystallogr.* **11**, 268-272.
- Pflugrath, J. W., Saper, M. A. & Quioco, F. A. (1984) in *Methods and Applications in Crystallographic Computing*, eds. Hall, S. & Ashida, T. (Clarendon, Oxford), pp. 404-407.
- Padlan, E. A., Davies, D. R., Pecht, I., Givol, D. & Wright, C. (1976) *Cold Spring Harbor Symp. Quant. Biol.* **41**, 627-637.
- Satow, Y., Cohen, G. H., Padlan, E. A. & Davies, D. R. (1986) *J. Mol. Biol.* **190**, 593-604.
- Brooks, B. R., Bruccoleri, R. E., Olafson, B. D., States, D. J., Swaminathan, S. & Karplus, M. (1983) *J. Comput. Chem.* **4**, 187-217.
- Connolly, M. L. (1983) *J. Appl. Crystallogr.* **16**, 548-558.
- Padlan, E. A. (1977) *Q. Rev. Biophys.* **10**, 35-65.
- Amzel, L. M. & Poljak, R. J. (1979) *Annu. Rev. Biochem.* **48**, 961-997.
- Chothia, C., Novotny, J., Bruccoleri, R. & Karplus, M. (1985) *J. Mol. Biol.* **186**, 651-663.
- Summers, N. L., Carlson, W. D. & Karplus, M. (1987) *J. Mol. Biol.* **196**, 175-198.
- Padlan, E. A., Cohen, G. H. & Davies, D. R. (1985) *Ann. Inst. Pasteur/Immunol.* **136**, 271-276.
- Glaudemans, C. P. J. (1986) *Mol. Immunol.* **23**, 917-918.
- Chothia, C., Lesk, A. M., Levitt, M., Amit, A. G., Mariuzza, R. A., Phillips, S. E. V. & Poljak, R. J. (1986) *Science* **233**, 755-758.
- Fine, R. M., Wang, H., Shenkin, P. S., Yarmush, D. L. & Levinthal, C. (1986) *Proteins: Struct. Funct. Genet.* **1**, 342-362.
- Benjamin, D. C., Berzofsky, J. A., East, I. J., Gurd, F. R. N., Hannum, C., Leach, S. J., Margoliash, E., Michael, J. G., Miller, A., Prager, E. M., Reichlin, M., Sercarz, E. E., Smith-Gill, S. J., Todd, P. E. & Wilson, A. C. (1984) *Annu. Rev. Immunol.* **2**, 67-101.
- Lemieux, R. V., Wong, T. C., Liao, J. & Kabat, E. A. (1984) *Mol. Immunol.* **21**, 751-759.
- Chen, H. T. & Kabat, E. A. (1985) *J. Biol. Chem.* **260**, 13208-13217.
- Chen, H. T., Kabat, E. A., Lundblad, A. & Ratcliffe, R. M. (1987) *J. Biol. Chem.* **262**, 13579-13583.
- Gooi, H. C., Hounsell, E. F., Picard, J. K., Lowe, A. D., Voak, D., Lennox, E. S. & Feizi, T. (1985) *J. Biol. Chem.* **260**, 13218-13224.
- Glaudemans, C. P. J. (1987) *Mol. Immunol.* **24**, 371-377.
- Kimura, H., Cook, R., Meek, K., Umeda, M., Ball, E., Capra, J. D. & Marcus, D. M. (1988) *J. Immunol.* **140**, 1212-1217.